Global-Scale Weekly and Monthly Energetics During January and February 1979

JAN PAEGLE

Department of Meteorology, University of Utah, Salt Lake City 84112

WAYMAN E. BAKER

Laboratory for Atmospheric Sciences, NASA/Goddard Space Flight Center, Greenbelt, MD 20771

(Manuscript received 18 January 1982, in final form 2 August 1982)

ABSTRACT

Time averages of the latitudinal distribution of kinetic energy and terms of the kinetic energy equation are presented as depicted by the Goddard Laboratory for Atmospheric Science (GLAS) analyses of the First GARP Global Experiment (FGGE) during the First Special Observing Period (SOP-1). Monthly averages display peaks in the stationary wave energy at 30°N and in the tropics. Global decompositions of the streamfunction and velocity potential in spherical harmonics are truncated at the fourth degree. The kinetic energy distribution of the associated wind field displays peaks in the tropics and northern mid-latitudes in January, but only a tropical peak in February.

The Eliassen-Palm relationship for latitudinal momentum and geopotential wave transport appears to have some support in these analyses, particularly in the mid-latitudes. In the deep tropics, latitudinal convergence of the *fully resolved* stationary wave momentum transport accompanies latitudinal *convergence* of stationary wave geopotential flux in westerly flow, in contradiction to this relationship.

Such results make it difficult to interpret time averages in terms of idealized wave propagation and linear theories. However, there is an interesting correspondence between observed weekly averages of the global-scale kinetic energy and the zonally averaged wind.

1. Introduction

The first part of this study (Paegle and Baker, 1982) presented synopses of the wind and mass fields during the first special observing period (SOP-1) of the first GARP (Global Atmospheric Research Program) global experiment (FGGE). A truncated spectral representation of the meridional flow in that study contains important divergent contributions whose vertical structure is suggestive of a strong heat generation. Moreover, the time changes of the divergent cross-equatorial flow and of the sub-tropical jet stream are compatible with suggestions of the importance of tropical heating in several earlier synoptic and theoretical studies (Bjerknes, 1966, 1969; Ramage, 1968; Webster, 1972; Krishnamurti *et al.*, 1973; Paegle *et al.*, 1979; Johnson *et al.*, 1981; and others).

Estimates of tropical latent heating (e.g., Newell *et al.*, 1974) suggest that the longitudinal gradients of tropical latent heating may be as large as the meridional gradients. Thus, the direct generation of available potential energy in longitudinal modes may be as great as the generation of the zonally averaged available potential energy. Nevertheless, on long time scales there is strong evidence that localized heat input in the tropics tends to warm the entire tropical band (e.g., Horel and Wallace, 1981), implying that tropical heating with significant longitudinal variation may produce an effectively zonal response in the field of available potential energy.

To the extent that localized heating in the tropics merely intensifies the entire Hadley cell and the zonally averaged circulation, the distribution of jet streams and storm tracks of extratropical latitudes is principally a consequence of extratropical topography and heating acting in combination with barotropic and baroclinic instability in ways that are rather insensitive to the particular placement of tropical monsoons. Conversely, if the longitudinal variation of tropical heating produces circulations that have a significant projection upon the longitudinal structure of the global modes, the extratropical wave pattern is also influenced by the regional distribution of tropical precipitation.

Diagnostic studies presented by Paegle *et al.* (1979) and observed wave momentum fluxes interpreted in terms of long-wave theory by Dickinson (1971) indicate a potentially important long-wave source in the deep tropics. However, linear models suggest that climatologically observed tropical critical latitudes effectively impede meridional propagation of Rossby wave modes (e.g., Bennett and Young, 1971; Hoskins *et al.*, 1977; Tung, 1979, Opsteegh and Van den Dool, 1980).

0022-4928/82/122750-10$06.50

Since a zero wind line (i.e., a critical latitude for stationary modes) commonly exists on the winter hemisphere side of the most intense tropical precipitation of the summer hemisphere, there is little theoretical basis for a strong connection between the most active tropical monsoons of the summer hemisphere and the semi-stationary long waves of the winter hemisphere. It is difficult to check the critical latitude theories with data sets that do not display transitions between states that contain critical latitudes and those that do not.

The FGGE data present a unique opportunity to test the theory because of the extensive data coverage, and because of a remarkable transition from westerly to easterly tropical flow during the SOP-1 period.

The purpose of the present study is to quantify meridional energy structure and propagation, as well as the momentum flux and time changes of zonally averaged wind. The simplest theories of meridionally propagating Rossby waves generally satisfy the Eliassen-Palm (1961) relation between momentum and geopotential fluxes. Over most of the globe, the SOP-1 data satisfy this relation, at least with respect to sign (Section 2). However, within the deep tropics this is not true, possibly because of local wave transience, energy dissipation or energy sources.

Global-scale fields, defined in terms of low-order spherical harmonic expansions, exhibit the best correlation between critical latitude trapping theories and zonal flow evolution (Section 3).

The explanation of the westerlies over the equator is an interesting problem. Zonally averaged westerlies at the equator cannot be explained by a symmetric Hadley cell model. Such flow can result only from the convergence of westerly momentum transport by waves. This convergence is quite strong during SOP-1 (Section 4) and may explain the equatorial westerlies during January 1979.

2. Kinetic energy maintenance

a. Kinetic energy equation

In this section we analyze the maintenance of the longitudinal structure of the time average flow. For this purpose it is convenient to define the longitudinal average of a quantity such as V as

$$\bar{\mathbf{V}} = \frac{1}{2\pi}\int_0^{2\pi} \mathbf{V}\,d\lambda, \tag{1}$$

where λ is longitude. $\bar{\mathbf{V}}$ is time, pressure and latitudinally (ϕ) dependent. Deviations of the total V field from $\bar{\mathbf{V}}$ are denoted by $\mathbf{V}'$ which is also longitudinally dependent. The flux form of the frictionless momentum equation is then

$$\frac{\partial}{\partial t}(\bar{\mathbf{V}}+\mathbf{V}') + \frac{1}{r\cos\phi}\frac{\partial}{\partial\lambda}[(\bar{u}+u')(\bar{\mathbf{V}}+\mathbf{V}')] + \frac{1}{r\cos\phi}\frac{\partial}{\partial\phi}[(\bar{v}+v')(\bar{\mathbf{V}}+\mathbf{V}')\cos\phi] + \frac{\partial}{\partial P}[(\bar{\omega}+\omega')(\bar{\mathbf{V}}+\mathbf{V}')] + f\mathbf{k}\times(\bar{\mathbf{V}}+\mathbf{V}') = -\nabla(\bar{\Phi}+\Phi'). \tag{2}$$

Here f is the Coriolis parameter, r the earth radius, and Φ the geopotential.

Performing the scalar product of the vector Eq. (2) with $\bar{\mathbf{V}}+\mathbf{V}'$, and averaging the result over longitude gives

$$\underbrace{\frac{\partial}{\partial t}(\overline{\mathrm{KE}}+\overline{\mathrm{KE}'})}_{\text{(a)}} + \underbrace{\frac{1}{r\cos\phi}\frac{\partial}{\partial\phi}\overline{(v'\cos\phi\mathrm{KE}')}}_{\text{(b)}} + \underbrace{\frac{1}{r\cos\phi}\frac{\partial}{\partial\phi}(\bar{v}\overline{\mathrm{KE}}\cos\phi)}_{\text{(c)}} + \underbrace{\frac{1}{r\cos\phi}\frac{\partial}{\partial\phi}(\bar{v}\overline{\mathrm{KE}'}\cos\phi)}_{\text{(d)}} + \underbrace{\frac{\partial}{\partial P}(\bar{\omega}\overline{\mathrm{KE}})}_{\text{(e)}} + \underbrace{\frac{\partial}{\partial P}(\overline{\omega'\mathrm{KE}'})}_{\text{(f)}} + \frac{1}{r\cos\phi}\frac{\partial}{\partial\phi}\times[\overline{\cos\phi v'(\bar{u}u'+\bar{v}v')}] + \underbrace{\frac{\partial}{\partial P}[\overline{\omega'(\bar{u}u'+\bar{v}v')}]}_{\text{(g)}\qquad\text{(h)}} = \underbrace{-\bar{\mathbf{V}}\cdot\nabla\bar{\Phi}}_{\text{(i)}} - \underbrace{\nabla\cdot(\overline{\mathbf{V}'\Phi'})}_{\text{(j)}} + \underbrace{\overline{\Phi'\nabla\cdot\mathbf{V}'}}_{\text{(k)}}. \tag{3}$$

Here

$$\mathrm{KE}' = (u'^2+v'^2)/2,$$
$$\overline{\mathrm{KE}} = (\bar{u}^2+\bar{v}^2)/2.$$

Term (a) represents the time change of kinetic energy, terms (b), (c), (d) and (g) the convergence of meridional energy transport, and terms (e), (f) and (h) the vertical energy transport. Term (i) which denotes the generation of kinetic energy by cross-isobaric flow in the mean, reduces to

$$-\bar{\mathbf{V}}\cdot\nabla\bar{\Phi} = -\frac{\bar{v}}{r\cos\phi}\frac{\partial\bar{\Phi}}{\partial\phi}.$$

Term (j) is the convergence of the pressure work by eddies and is sometimes also referred to as the convergence of potential energy. It can be written as

$$-\nabla\cdot(\overline{\mathbf{V}'\Phi'}) = -\frac{1}{\cos\phi}\frac{\partial}{\partial\phi}(\overline{v'\Phi'}\cos\phi).$$

Term (k) contains the vertical pressure work term together with the baroclinic conversion term $-\alpha'\omega'$. It can be written as

$$\overline{\Phi'\nabla\cdot\mathbf{V}'} = -\frac{\partial(\overline{\Phi'\omega'})}{\partial P} - \overline{\alpha'\omega'},$$

where α' is the specific volume.

In this study we compute the meridional fluxes of energy corresponding to the terms (b), (c), (d), (g) and (j) of Eq. (3). This is performed using weekly and monthly averaged values of V and Φ in order to study the meridional coupling of stationary modes. Therefore, we do not discuss the extra terms due to correlations of time transients that arise when Eq. (3) is averaged in time.

b. *Monthly averages*

The subsequent diagnostic calculation of the global-scale energetics presented below is based upon analyses of FGGE SOP-1 produced by the GLAS analysis forecast system described by Halem *et al.* (1982) and utilized by Paegle and Baker (1982).

Fig. 1 presents the latitudinal distribution of $\overline{KE'}\cos\phi$ at various pressure levels for January and February. Each month presents relative maxima around the equator and near 30°N. The tropical maximum diminishes by about 8% from January to February, and the maximum around 30°N decreases by more than 30% between the two months. Fig. 2 presents the meridional flux of eddy kinetic energy associated with terms (b) and (d) of Eq. (3). The fluxes are strongest at 200 mb, but even at this level the magnitudes are much weaker than those of the pressure work term ($\overline{v'\Phi'}\cos\phi$) shown in Fig. 3.

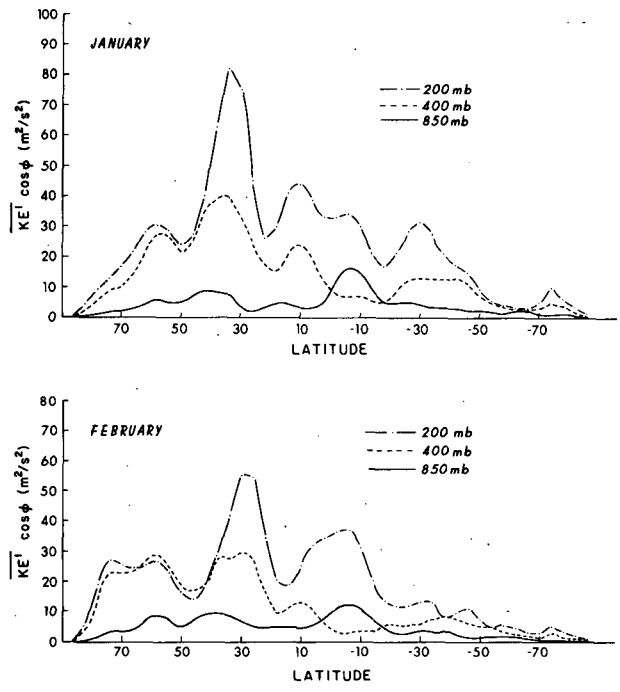

FIG. 1. Latitudinal distribution of wave kinetic energy per unit mass.

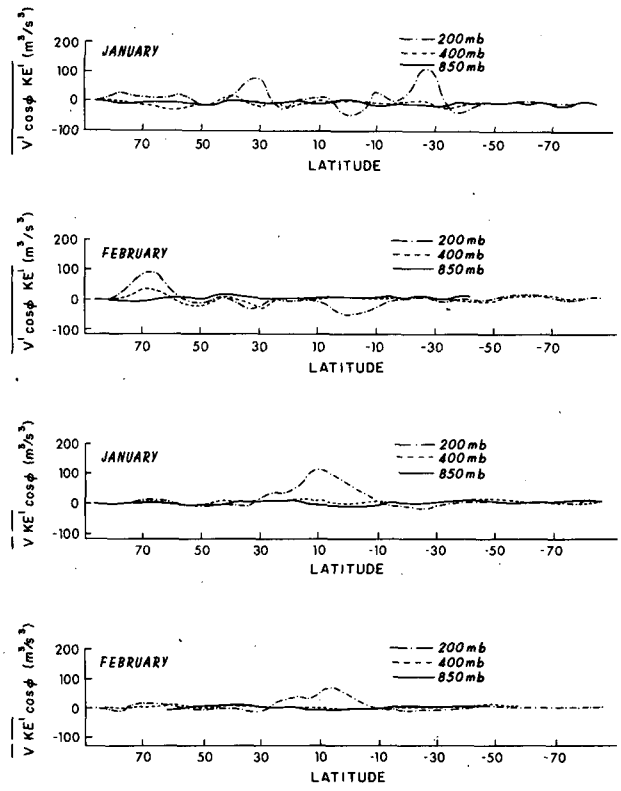

FIG. 2. Latitudinal distribution of the fluxes associated with terms (b) and (d) of Eq. (3).

The strong divergence of $\overline{v'\Phi'}\cos\phi$ out of the mid-latitudes (30–50°N) would deplete this region of an amount of wave kinetic energy equal to the January average in about two days. The maintenance of the standing wave pattern must therefore be a consequence of sources that counteract this depletion. Likely possibilities include advection, baroclinic instability, and topographic and other surface inhomogeneities.

Conversely, in the belt from 30°N to the equator, the meridional convergence of $\overline{v'\Phi'}\cos\phi$ is sufficient to double the wave kinetic energy density in about two days. The only other contribution of roughly comparable magnitude of Eq. (3) is term (g).

Fig. 4 presents the January latitudinal distribution of $\bar{u}(\overline{u'v'})\cos\phi$ [the dominant contribution to term (g) in Eq. (3) at 200 mb]. For reference, the latitudinal variation of $\overline{v'\Phi'}\cos\phi$ and $(\bar{v}+v')\overline{KE'}\cos\phi$ [corresponding to terms (j) and (b + d), respectively] at 200 mb are also shown. The tendency for cancellation in the sum

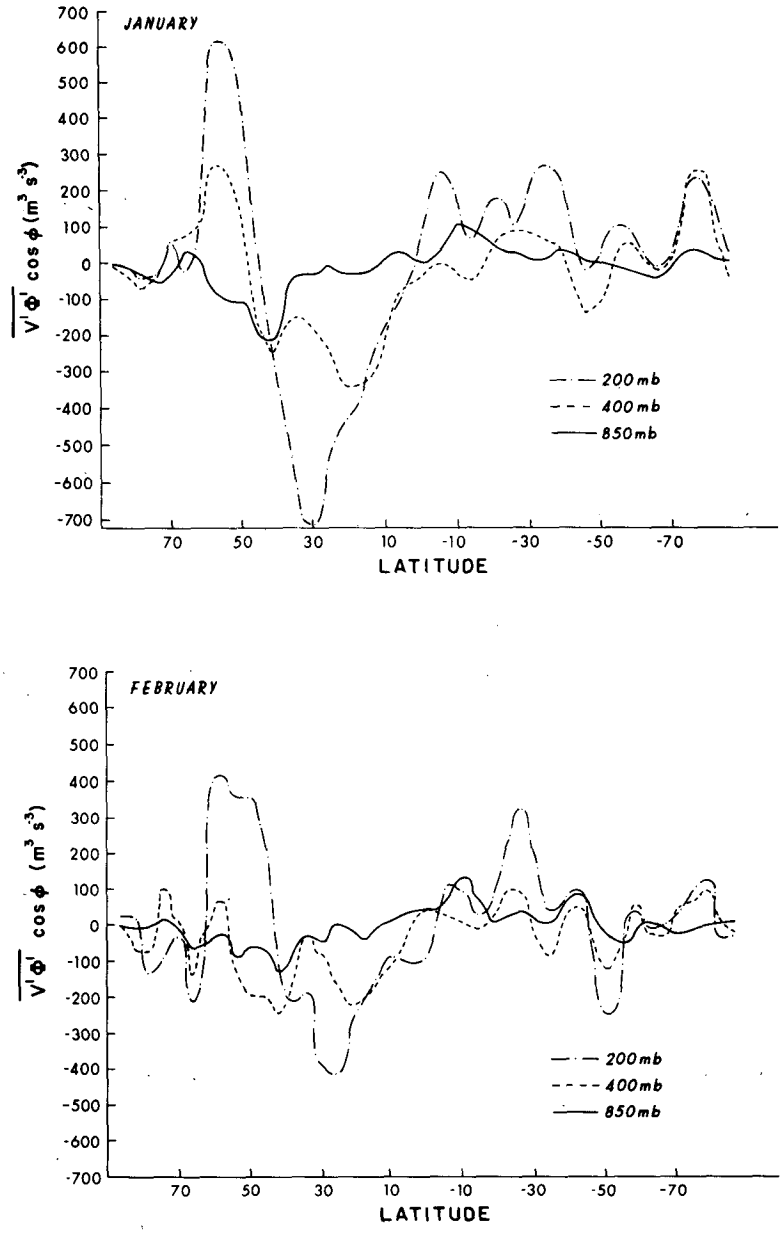

FIG. 3. Latitudinal distribution of the fluxes associated with term (j) of Eq. (3).

$$\bar{u}(\overline{u'v'}) + \overline{v'\Phi'}$$

is quite obvious. Thus, at least to a crude approximation, the simplest version of the relationship between meridional energy and momentum fluxes

$$\overline{v'\Phi'} = -\bar{u}(\overline{u'v'}) \qquad (4)$$

suggested by Eliassen and Palm (1961), which is strictly valid only for linearized, unforced, non-dissipative, stationary waves, appears to have some relevance for monthly averaged SOP-1 data at 200 mb. One conspicuous contradiction to this theory occurs near the equator where convergence of both $\overline{v'\Phi'}$ and $\overline{u'v'}$ occur with positive $\bar{u}$ (Fig. 5).

The terms of Eq. (4) are the dominant second-order products in the more complete relation given by Eq. (3). The third-order products (e.g., $\overline{v'\mathrm{KE}'}\cos\phi$) of Eq. (3) are systematically weaker, while individual mean contributions (e.g. $\bar{v}\overline{\mathrm{KE}}\cos\phi$) possess similar magnitudes to the terms in Eq. (4).

The present situation is quite different from the one described for the DST period of winter 1976 by Paegle *et al.* (1979). In that study, the region from about 20°S to 20°N was a source rather than a sink

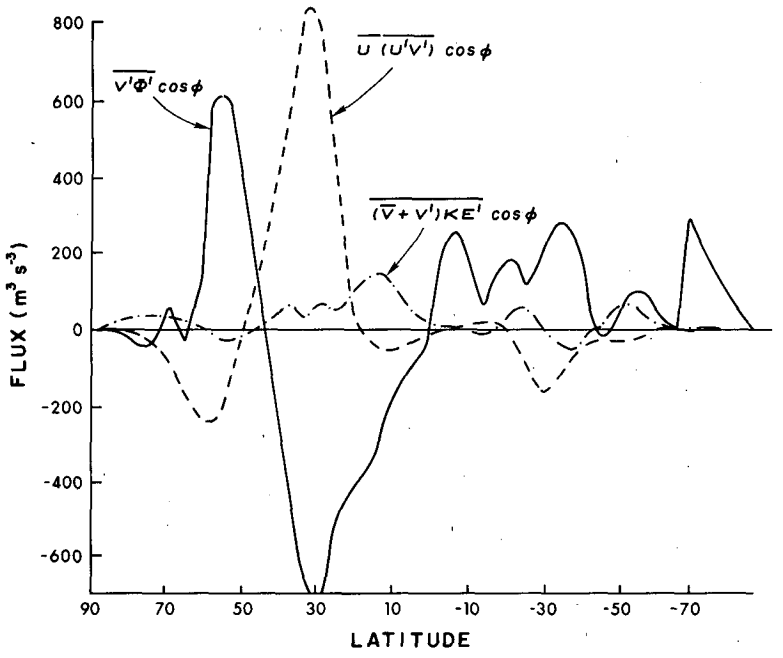

FIG. 4. Latitudinal distributions of fluxes associated with terms (b), (d), (g), (j) of Eq. (3) at 200 mb.

for the pressure work terms. A likely explanation for this discrepancy is that the data coverage in the tropics for the DST analyses investigated by Paegle *et al.* (1979) was not as complete as the coverage of the present data.

Another possible explanation for the difference between SOP-1 data presently described and the winter 1976 DST data is that the meridional energy flux is strongly dependent upon the horizontal scale, and the dominant observed scale may be different for different periods or different data densities. Fig. 5 displays the pressure work term obtained from a spectral triangular truncation (at degree 4) of the streamfunction, velocity potential and geopotential expanded in a series of spherical harmonics. Fig. 5 shows more flux out of the tropics than does Fig. 3. The latitudinal variation of $\overline{KE'}$ resolved to this truncation is quite different between January and February (Fig. 5). Whereas January contains two maxima (at about 40°N and 10°S), February only displays the tropical maximum.

c. *Relation to the zonal flow*

One of the useful conclusions from Eq. (4) is that no work is done by waves across the approximate latitude at which $\bar{u} = 0$ (the "critical latitude"). A large body of theory holds that critical latitudes may effectively impede meridional propagation of standing wave energy.

Fig. 6 displays the latitudinal structure of the zonally averaged flow for January. At 400 and 200 mb the winds are westerly at all latitudes, while easterlies are found at 850 mb from about 30°S to 22°N. Fig. 7 shows the change in this field from January to February. The greatest changes occur in the upper troposphere of the tropics and polar regions. In the for-

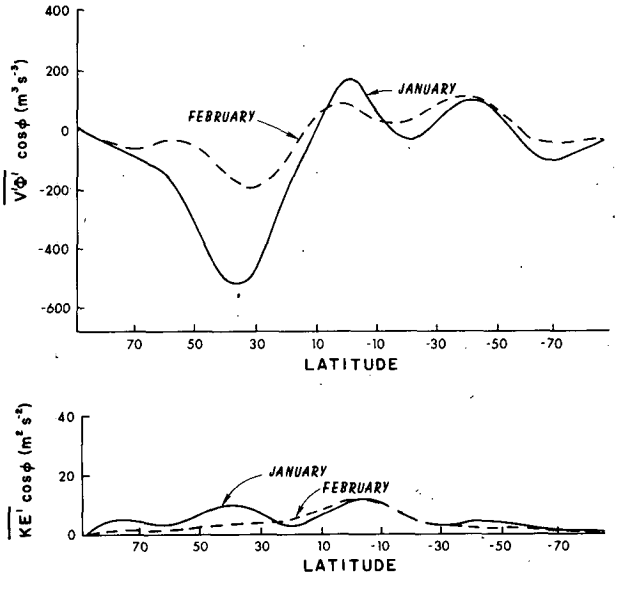

FIG. 5. TOP: latitudinal distribution of the 200 mb meridional pressure work term for a triangular truncation in a spherical harmonic expansion neglecting terms past the fourth degree for the streamfunction, velocity potential and geopotential. BOTTOM: latitudinal distribution of the 200 mb wave kinetic energy displayed to a similar truncation.

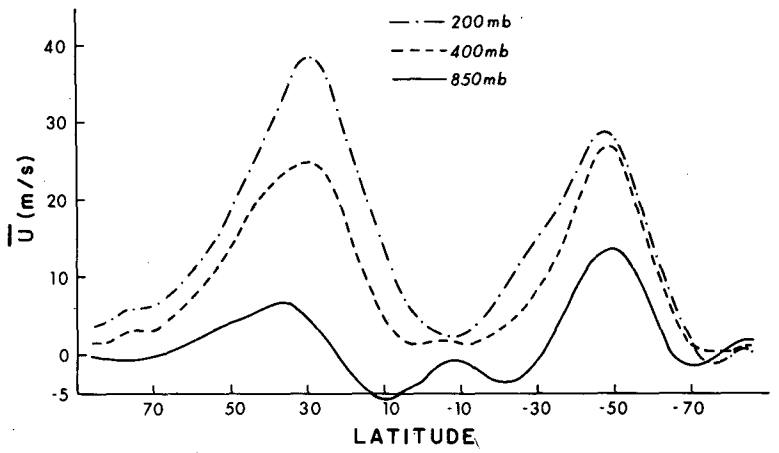

FIG. 6. Latitudinal distribution of the longitudinally averaged zonal wind for January.

mer region the westerlies diminish by about 5 m s^{-1}, while in the latter they increase by about this much. This change produces equatorial easterlies throughout the troposphere during February.

To the extent that linear theory holds, (e.g., Bennett and Young, 1971; Hoskins *et al.*, 1977; Opsteegh and Van den Dool, 1980) the wave activity of the Northern and Southern Hemispheres should be more effectively insulated during February than during January. The mid-latitude standing wave energy of Figs. 1 and 5 does diminish rather markedly from January to February, while the tropical wave energy is more nearly preserved.

3. Weekly variations

Weekly averages of $\bar{u}$ also display notable changes. The minimum upper tropospheric value of $\bar{u}$ is generally located between 6 and 10°S. The average minimum zonal wind ($\bar{U}_m$) is plotted in Fig. 8 for each week at 200 mb. It changes from westerly to easterly between the fourth and fifth weeks, and a critical latitude is found near the equator each of the final four weeks.

The week-to-week variations of the wave kinetic energy are as great as the month-to-month variations, with the changes in the low-order global scales being especially pronounced. Fig. 9 displays the latitudinal distribution of the kinetic energy of weekly averaged globally truncated flow fields (i.e., computed from a spectral triangular truncation, at degree 4, of the streamfunction and the velocity potential) for eight consecutive weeks beginning 5 January 1979. In equatorial regions, there is a local maximum of 20 m^2 s^{-2} during the second week, which diminishes to about 10 m^2 s^{-2} during the seventh week. At about

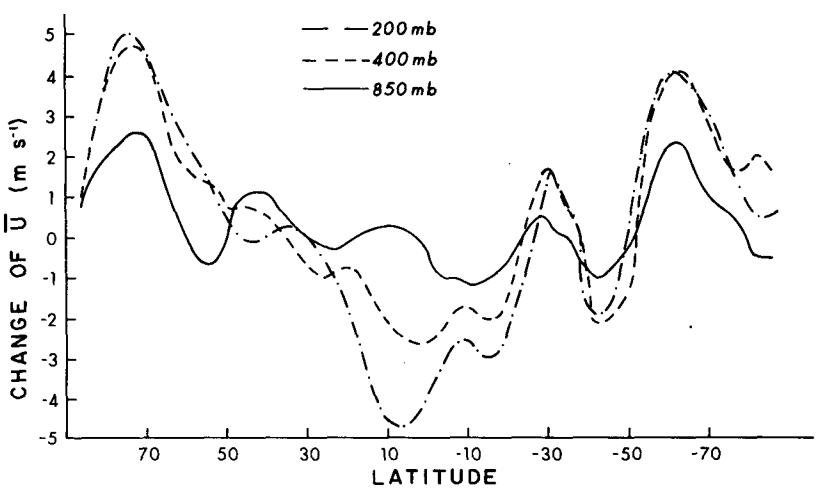

FIG. 7. Latitudinal distribution of the change of the longitudinally averaged zonal wind from January to February (February − January).

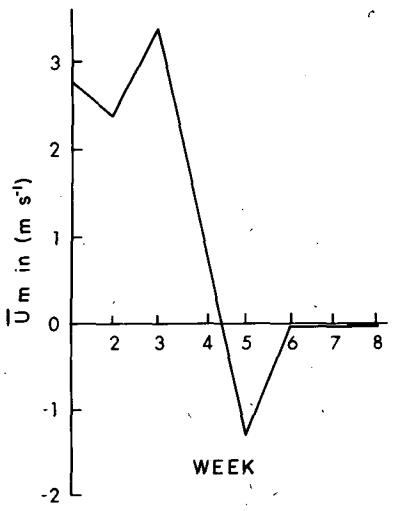

FIG. 8. The weekly variation of the minimum zonally averaged zonal wind component at 200 mb for the first eight weeks of SOP-1.

45°N, the maximum value is 19 $m^2 s^{-2}$ during the third week, which diminishes to about 2 $m^2 s^{-2}$ during the sixth week.

The mid-latitude fluctuations of this pattern are greater than those at low latitudes, and the energy of the last four weeks is rather effectively trapped in the tropics. The pressure work term at the same truncation is displayed in Fig. 10. Enhanced tropical sources of the second week subside during the third week, and remain rather reduced the remainder of the period.

To the extent that critical latitudes inhibit latitudinal propagation of weekly averaged wave fields, we may expect more regional trapping during the last four weeks than during the first four weeks of SOP-1. Moreover, the latitudes of strongest excitation should display greatest wave energy during the trapped episodes. Since a tropical energy peak in the largest scales occurs each week, whereas enhanced mid-latitude wave activity to this truncation is present only during episodes of westerly tropical flow, critical latitude trapping is plausible if the kinetic energy source for these modes is located in the tropics.

4. Maintenance of tropical westerlies

The longitudinally averaged zonal component of Eq. (2) is

$$\frac{d\bar{u}}{dt} + f\bar{v} = -\frac{1}{r\cos\phi}\frac{\partial}{\partial\phi}(\overline{v'u'}\cos\phi) - \frac{\partial}{\partial P}(\overline{\omega'u'}). \quad (5)$$

In the absence of waves, Eq. (5) indicates that the angular momentum of the flow is conserved, implying that equatorial westerlies are impossible if at some point the flow does not possess angular momentum larger than that of the earth's surface at the equator. Symmetric models of the Hadley circulation, which

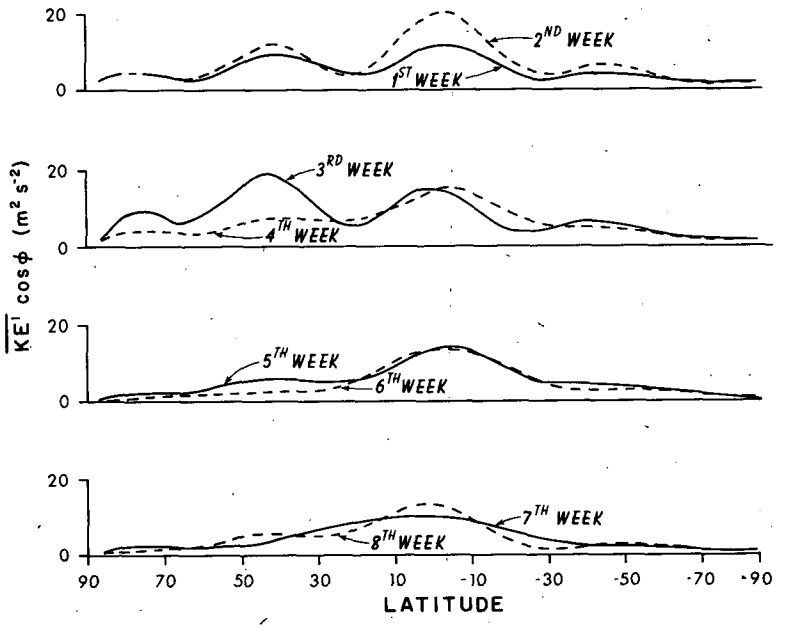

FIG. 9. Latitudinal distribution of the kinetic energy associated with the longitudinally variable portion of the motion field obtained from a triangular truncation of a spherical harmonics expansion of the streamfunction and velocity potential neglecting terms past the fourth degree.

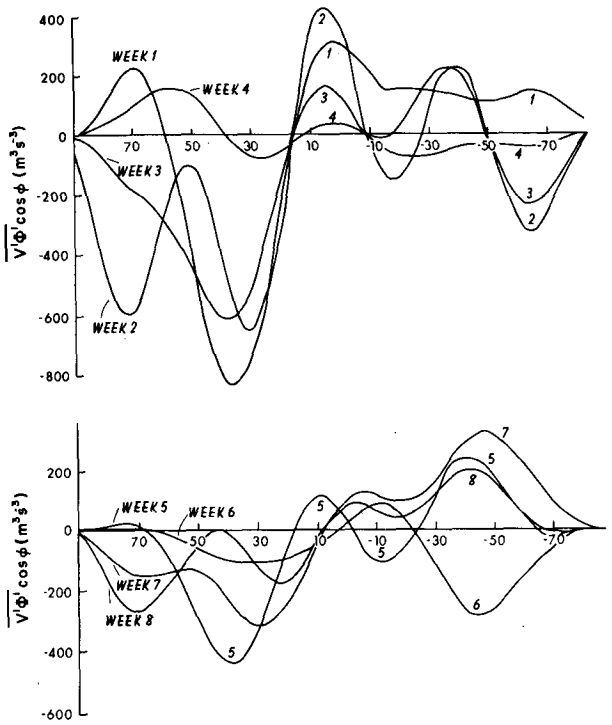

FIG. 10. Latitudinal distribution of the 200 mb wave pressure work term calculated to the same truncation as described in Fig. 8. The first eight weeks of SOP-1 are shown.

include non-adiabatic terms, also exhibit tropical easterlies at all levels.

Tropical westerlies may be accelerated by systematic convergence of westerly momentum transport by waves. This may occur through meridional transport or through vertical transport. Fig. 11 displays the latitudinal distribution of the monthly averaged patterns. Convergence of the westerly wave momentum transport is quite apparent each month from about 2°N to about 14°S. Both periods display sufficient convergence of 200 mb standing wave momentum to accelerate $\bar{u}$ by about 20 m s^{-1} in one month in the belt from the equator to 10°S. However, at the equator there is convergence of westerly momentum for the column average during January but not during February.

Thus, the upper tropospheric tropical westerlies during January may be produced, at least in part, by the systematic meridional convergence of westerly momentum transport by standing waves. While the distinctions of the transport field between January and February are rather minor, they are qualitatively consistent with the monthly distribution of westerlies and easterlies, at least in the immediate vicinity of the equator.

The maintenance of equatorial westerlies against dissipation requires sustained convergence of westerly momentum. This is consistent with the Eliassen-Palm relation only if a source of geopotential wave flux exists around the equator. Such a source means that the tropical atmosphere is performing pressure work upon the surroundings, which implies a tropical energy source.

The possibility of enhanced tropical sources during January is supported by the northward geopotential flux across the equator in January that becomes significantly weaker in February (see Fig. 3 for the full fields and Fig. 10 for the global-scale weekly evolution).

5. Conclusions

The major results of the present study may be summarized as follows:

- The stationary wave patterns during both January and February possess significant energy peaks around 30°N and in the deep tropics with the subtropical peak being about 50% stronger in January than in February.
- The zonally averaged zonal wind is westerly in the upper troposphere at all latitudes, including the equator during January, but becomes easterly around the equator in February.
- The pressure work term of the fully resolved sta-

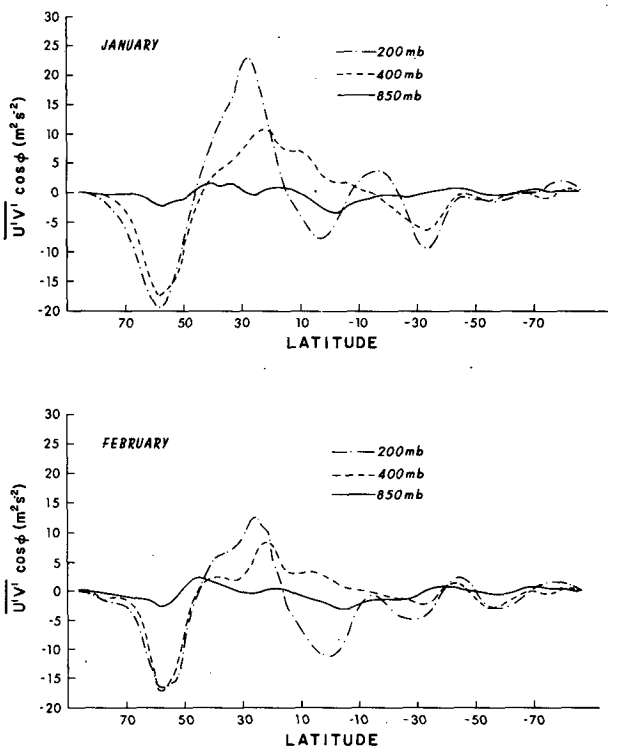

FIG. 11. Latitudinal variation of the meridional momentum flux for the time-averaged flows of SOP-1 during January and February.

tionary energy spectrum displays strong convergence into the tropics both months and a simple verification of the critical latitude theories in terms of these data and the Eliassen-Palm relation is not clearly evident, probably because of local transience, dissipation and energy sources. If linear critical latitude theories were applied, we would conclude that the more energetic mid-latitude month of January would be explained by greater tropical forcing from which the higher latitudes would not be shielded by a critical latitude as in February. The alternate conclusion, that there is a stronger flux of mid-latitude energy into low latitudes in January than in February, does not have obvious support, because tropical waves are not much stronger in January than in February.

- The global scale components of a spherical harmonics decomposition of the fields display more obvious conformity with critical latitude theories, for a triangular truncation at wavenumber 4. The following inferences are supported by the upper tropospheric components of such a representation.
- The tropical kinetic energy increases during the first two weeks of SOP-1. This increase helps to explain a concomitant increase of tropical westerlies due to local convergence of wave momentum flux that appears to be consistent with Eliassen and Palm's (1961) theorem and an increase in the pressure work term out of the tropics. The third week of SOP-1 shows a strong mid-latitude peak of long-wave energy that may reflect the propagation of the tropical energy into higher latitudes. Perhaps somewhat coincidentally, a strong North Atlantic block appears at this time. As the tropical wave activity diminishes during the subsequent weeks, the pressure work term decreases and the long-wave energy within high latitudes decays to about 30% of its prior peak value.

This picture of tropical generation of global-scale wave structure, meridional propagations and zonal winds has been suggested for a rather highly truncated form of the total field that contains only ~25% of the total stationary wave kinetic energy in midlatitudes and ~40% of the total stationary wave kinetic energy in the tropics. At least some (and perhaps most) of the remaining energy is in modes for which baroclinic and barotropic instabilities, along with topographic effects, have been shown to be dominant in other studies. It would be useful to ascertain the spectral truncation at which the self-consistent, tropically forced idealizations, in terms of essentially linearized theories, become obscured (as in the full spectrum). Additionally, since the spherical harmonics have limited physical content, it would be useful to perform the expansions in terms of eigenfunctions of the tidal equations.

The present conclusions depend upon data reliability and analysis, and may also be affected by neglected transient terms. The SOP-1 FGGE data represent the most complete global data set yet available. Our emphasis of the upper troposphere is partly motivated by the high data density (especially aircraft winds and cloud motion vectors), the stronger physical signal, and the relevance of the upper troposphere in meridional interactions suggested in other investigations (Paegle *et al.*, 1979; Opsteegh and Van den Dool, 1980; Hoskins and Karoly, 1981). The focus upon time-averaged fields is motivated by the fundamental importance of quasi-stationary components, both to theory and application, as well as the greater reliability of time-averaged analyses.

Our comparisons of the GLAS analysed fields with ECMWF analyses indicate reasonable agreement even for the divergent wind. However, it would be most useful to repeat at least some of the present calculations with other analyses to gain an impression of the sensitivity to the analysis scheme. It would also be useful to do this on an analysis based upon a reduced data set, in order to ascertain the sensitivity to data density. Finally, the calculations of the available potential energy, transient terms, vertical fluxes and vertical integrals should also be performed to complete the diagnostic picture.

Acknowledgments. We wish to acknowledge Dr. Milton Halem for his continuing support and encouragement of this work. We would especially like to thank Dr. Eugenia Kalnay for many helpful suggestions and comments on the manuscript. We also acknowledge the substantial assistance of Mr. D. Edelmann for computational and technical support; Messrs. S. Breining and M. Iredell with graphics and data, and Ms. A. Johnson for typing the manuscript. Part of this research was supported under NASA Grant NAG 5-127.

This research was performed while one of us (JP) was supported by a National Research Council Fellowship at GLAS.

REFERENCES

Bennett, J. R., and J. A. Young, 1971: The influence of latitudinal wind shear upon large-scale wave propagation into the tropics. *Mon. Wea. Rev.*, **99**, 202–214.

Bjerknes, J., 1966: A possible response of the atmospheric Hadley circulation to equatorial anomalies of ocean temperature. *Tellus*, **18**, 820–829.

——, 1969: Atmospheric teleconnections from the equatorial Pacific. *Mon. Wea. Rev.*, **97**, 163–172.

Dickinson, R. E., 1971: Cross equatorial eddy momentum fluxes as evidence of tropical planetary wave sources. *Quart. J. Roy. Meteor. Soc.*, **97**, 554–558.

Eliassen, A., and E. Palm, 1961: On the transfer of energy in stationary mountain waves. *Geofys. Publ.*, **22**, No. 3, 1–23.

Halem, M., E. Kalnay, W. E. Baker and R. Atlas, 1982: An assessment of the FGGE satellite observing system during SOP-1. *Bull. Amer. Meteor. Soc.*, **63**, 407–426.

Horel, J. D., and J. M. Wallace, 1981: Planetary-scale atmospheric phenomena associated with the Southern Oscillation. *Mon. Wea. Rev.*, **109,** 813–829.

Hoskins, B. J., A. J. Simmons and D. G. Andrews, 1977: Energy dispersion in a barotropic atmosphere, *Quart. J. Roy. Meteor. Soc.*, **103,** 553–568.

——, and D. J. Karoly, 1981: The steady linear response of a spherical atmosphere to thermal and orographic forcing. *J. Atmos. Sci.*, **38,** 1179–1196.

Johnson, D. R., R. D. Townsend, M. Y. Wei and R. D. Selin, 1981: The global structure of energy transport within thermally-forced planetary-scale mass circulations. *International Results of FGGE and its Monsoon Experiment.* WMO Report, 3-27 to 3-34.

Krishnamurti, T. N., M. Kanamitsu, W. J. Koss and J. D. Lee, 1973: Tropical east-west circulations during the northern winter. *J. Atmos. Sci.*, **30,** 780–787.

Newell, R. E., J. W. Kidson, D. G. Vincent and G. J. Boer, 1974: *The General Circulation of the Tropical Atmosphere and Interactions with Extratropical Latitudes.* The MIT Press, Cambridge, 371 pp.

Opsteegh, J. D., and H. M. Van Den Dool, 1980: Seasonal differences in the stationary response of a linearized primitive equation model: Prospects for long range weather forecasting? *J. Atmos. Sci.*, **37,** 2169–2185.

Paegle, J., J. N. Paegle, F. P. Lewis and A. J. McGlasson, 1979: Description and interpretation of planetary flow structure of the winter 1976 DST data. *Mon. Wea. Rev.*, **107,** 1506–1514.

——, and W. E. Baker, 1982: Planetary-scale characteristics of the atmospheric circulation during January and February 1979. *J. Atmos. Sci.*, **39,** 2521–2538.

Ramage, C. S., 1968: Role of a tropical "maritime continent" in the atmospheric circulation. *Mon. Wea. Rev.*, **96,** 365–370.

Tung, K. K., 1979: A theory of stationary long waves. Part III: Quasi-normal modes in a singular waveguide. *Mon. Wea. Rev.*, **107,** 751–774.

Webster, P. J., 1972: Response of the tropical atmosphere to local steady forcing. *Mon. Wea. Rev.*, **100,** 518–541.